

## A Membrane-proximal Basic Domain and Cysteine Cluster in the C-terminal Tail of CCR5 Constitute a Bipartite Motif Critical for Cell Surface Expression\*

Received for publication, June 20, 2001, and in revised form, July 24, 2001  
Published, JBC Papers in Press, August 20, 2001, DOI 10.1074/jbc.M105722200

Sundararajan Venkatesan<sup>‡§</sup>, Ana Petrovic<sup>‡</sup>, Massimo Locati<sup>¶</sup>, Yong-Ou Kim<sup>‡</sup>, Drew Weissman<sup>¶</sup>, and Philip M. Murphy<sup>¶</sup>

From the <sup>‡</sup>Laboratory of Molecular Microbiology and <sup>¶</sup>Laboratory of Host Defenses, NIAID, National Institutes of Health, Bethesda, Maryland 20892 and the <sup>§</sup>Division of Infectious Diseases, University of Pennsylvania, Philadelphia, Pennsylvania 19104

We examined the structural requirements for cell surface expression, signaling, and human immunodeficiency virus co-receptor activity for the chemokine receptor, CCR5. Serial C-terminal truncation of CCR5 resulted in progressive loss of cell surface expression; mutants truncated at the 317th position and shorter were not detected at the cell surface. Alanine substitution of basic residues in the membrane-proximal domain (residues 314–322) in the context of a full-length C-tail resulted in severe reduction in surface expression. C-terminal truncation that excised the three cysteines in this domain reduced surface expression, but further truncation of upstream basic residue(s) abolished surface expression. Substituting the carboxyl-terminal domain of CXCR4 for that of CCR5 failed to rectify the trafficking defect of the tailless CCR5. In contrast, tailless CXCR4 or a CXCR4 chimera that exchanged the native cytoplasmic domain for that of wild type CCR5 was expressed at the cell surface. Deletion mutants that expressed at the cell surface responded to chemokine stimulation and mediated human immunodeficiency virus entry. Substitution of all serine and threonine residues in the C-terminal tail of CCR5 abolished chemokine-mediated receptor phosphorylation but preserved downstream signaling ( $\text{Ca}^{2+}$  flux), while substitutions of tyrosine residues in the C-tail affected neither phenotype. CCR5 mutants that failed to traffic to the plasma membrane did not exhibit obvious changes in metabolic turnover and were retained in the Golgi or pre-Golgi compartments(s). Thus, the basic domain (-KHIAKRF-) and the cysteine cluster (-CKCC-) in the C-terminal tail of CCR5 function cooperatively for optimal surface expression.

CCR5 is a member of the chemokine receptor subclass of the G protein-coupled receptor (GPCR)<sup>1</sup> superfamily (1). CCR5 reg-

ulates leukocyte chemotaxis in inflammation (2) and serves as a co-receptor for macrophage-tropic HIV entry (3–6). Expression of chemokine receptors is regulated at the transcriptional level in many cell types (1, 7–9). In addition, as members of GPCR family, they share a common three-dimensional architecture composed of seven transmembrane (TM) domains arranged in a counter-clockwise toroidal conformation, which defines multiple extracellular and intracellular loops (10–12). They possess extracellular N termini of variable length and a C-terminal cytoplasmic domain containing unique motifs critical for ligand-dependent receptor signaling, internalization, and desensitization (13, 14). These architectural requirements and the need to interact precisely with cellular components pertinent to receptor function may subject them to post-translational regulatory mechanisms. Specifically, intracellular trafficking of some GPCRs may reflect the need for specific cellular helper proteins to facilitate maturation and transport that may underlie their tissue-specific expression. Transport of some chemokine receptors such as CCR2A is restricted by *cis*-negative retention signals in the receptor tail (15). This may not be the case for CCR2B, CXCR2, or CXCR4, since C-terminal truncation of these receptors has little or no effect on cell surface expression (16–23).

Several natural mutations of CCR5 have shed some light on the multiple levels of regulation for this receptor. Besides mutations in the promoter region that have been correlated with transcriptional regulation (24–29), changes in the coding sequence also impact negatively on the surface expression of CCR5. Among the latter is the well characterized 32-base pair deletion mutant (CCR5  $\Delta$ 32) that is sequestered in the cytosol and in the homozygous state bestows complete resistance to M-tropic HIV infection (30–33). A naturally occurring 24-base pair in frame deletion in CCR5 from red-capped mangabeys was defective for  $\beta$ -chemokine-dependent signaling and might affect simian immunodeficiency virus pathogenesis (34). Analysis of 16 naturally occurring variants of CCR5 identified mutation at cysteine at 20, 102, or 178 that may disrupt potential extracellular disulfide loops and prevent ligand or antibody binding and a frameshift mutant at position 299 that was defective for cell surface trafficking (35). The role of the C-tail of CCR5 in surface expression, signaling and HIV usage has

\* The costs of publication of this article were defrayed in part by the payment of page charges. This article must therefore be hereby marked "advertisement" in accordance with 18 U.S.C. Section 1734 solely to indicate this fact.

§ To whom correspondence should be addressed: LMM, NIAID, Bldg. 10, Rm. 6A05, National Institutes of Health, Bethesda, MD 20892-1576. Tel.: 301-496-6359; Fax: 301-402-4122; E-mail: aradhana@helix.nih.gov.

<sup>1</sup> The abbreviations used are: GPCR, G protein-coupled receptor; APC, allophycocyanin; ER, endoplasmic reticulum; FITC, fluorescein 5-isothiocyanate; HIV, human immunodeficiency virus; ICL, intracellular loop; mAb, monoclonal antibody; MFV, mean fluorescence value; M-tropic, macrophage tropic; PAGE, polyacrylamide gel electrophoresis; PBS, phosphate-buffered saline; PE, phycoerythrin; TC, tricolor;

TM, transmembrane; TRITC, tetramethylrhodamine-5-(and -6)-isothiocyanate; WT, wild type; PCR, polymerase chain reaction; FCS, fetal calf serum; FACS, fluorescence-activated cell sorting; BSA, bovine serum albumin; CHAPS, 3-[(3-cholamidopropyl)dimethylammonio]-1-propanesulfonic acid; RANTES, regulated on activation normal T cell expressed and secreted; aa, amino acid(s); IL, interleukin; TGN, trans-Golgi network.

also been examined more directly. Truncation of the terminal carboxyl-tail to eight amino acids blocked chemokine-dependent activation of intracellular calcium flux and the cellular response of chemotaxis but not the ability to act as HIV-1 co-receptor (36, 37). Another report showed that a CCR5 mutant lacking the last 45 amino acids of the cytoplasmic C terminus (CCR5<sub>306</sub>) was expressed on transfected cells and displayed normal chemokine binding affinity and HIV co-receptor activity. However, it was defective for ligand-induced signaling (38). In contrast, Shioda *et al.* (40) have shown that a natural variant of CCR5, CCR5-893(-), observed exclusively in Asians (39), lacked the C-tail and was impaired for surface expression, being retained in the ER.

In this report, we have examined the structural elements in the carboxyl-terminal domain of CCR5 required for optimal surface expression. We have identified a membrane-proximal basic domain that is absolutely required for the transport of the receptor to the cell surface. This basic domain together with a neighboring cysteine cluster that has been recently identified to be palmitoylated (41) constitutes a bipartite motif required for the optimal transport and expression of CCR5.

#### MATERIALS AND METHODS

**Expression Plasmids**—Construction of the Rous sarcoma virus long terminal repeat- or cytomegalovirus immediate early promoter-linked expression plasmids for WT CCR2B, CCR3, CCR5, CXCR1, CXCR2, and CXCR4 have been described (3, 38, 42–44). The various mutants described in this paper were constructed *in vitro* by the overlap PCR method (45) and cloned using a commercial vector, pCDNA3.1 directional TOPO vector (Invitrogen Corp., Rockville, MD). Some of the mutants were also cloned into FLAG vector (Sigma) that appended a FLAG epitope at the N terminus of the indicated receptors.

**DNA Transfection**—Monolayers were transfected by the CaCl<sub>2</sub> method (Promega Corp., Madison, WI) or by lipofection using Eugene (Roche Molecular Biochemicals). The JJK line of Jurkat T cells (contributed by Dan Littman, Columbia University) in RPMI medium containing 10% FCS was transfected by use of a Bio-Rad electroporator (Bio-Rad) at a setting of 250 V and 960 microfarads.

**HIV Infectivity Measurement**—Pseudotyped HIV stocks expressing firefly luciferase in place of Nef were prepared by transfecting 293-T cells (by CaCl<sub>2</sub> precipitation) with 5 µg each of defective HIV provirus, pNL4-3 Env(-), vpR(-), luciferase(+), and plasmids encoding HIV-JRFL or avian myeloblastosis virus env (obtained through the National Institutes of Health (NIH) AIDS Research and Reference Reagent Program, Rockville, MD). Virus collected in the culture supernatants was quantified by reverse transcriptase assay and adjusted to constant reverse transcriptase units/ml.

293-T cells were transfected (by the CaCl<sub>2</sub> method) with CD4 alone or with a mixture of CD4 and the indicated CCR5 plasmid and harvested 36 h later. After checking the transfection efficiency by FACS analysis, CD4+ cells were purified by binding to and elution from CD4 antibody-coated magnetic beads using a commercial kit (Dynal Inc., Lake Success, NY) that resulted in recovery of >90% CD4+ cells. Eluted cells were seeded into 48-well plates (0.5–1 × 10<sup>5</sup> cells/well) and infected in triplicate with the respective pseudotyped luciferase-expressing HIVs. About 24–30 h after infection, cell lysates were assayed for luciferase activity using a commercial kit (Promega Corp., Madison, WI) and a microplate luminometer (Multex, Dynex Technologies, Chantilly, VA).

**Antibody Binding and Flow Cytometric Analysis**—The following monoclonal antibodies (mAbs) or rabbit antisera were used to identify the various chemokine receptors: 1) for CCR2, mAb, clone 48607 (R & D Systems, Minneapolis, MN); 2) for CCR3, FITC- or PE-conjugated rat mAb, clone 61828 (R & D Systems, Minneapolis, MN), mouse mAb 7B1 (NIH AIDS Research and Reference Reagent Program); 3) for CCR5, FITC- or APC-conjugated mAb 2D7, PE-conjugated mAb 3A9 (BD-Pharmingen, San Diego, CA), FITC-conjugated mAbs 181 and 182 (R & D Systems), unconjugated mAbs 2D7, 3A9, 5C7, 180, 181, 182, and 183 (NIH AIDS Research and Reference Reagent Program), and rabbit antibody against the N-terminal end of CCR5 (38); 4) for CXCR1, FITC- or PE-conjugated mAb, clone 42705 (R & D Systems), or unconjugated anti-CXCR1 antibody CDw128 (BD-Pharmingen, San Diego, CA); 5) for CXCR2, FITC- or PE-conjugated mAb, clone 48311 (R & D Systems) or unconjugated mAb, IL-8-Rb (BD-Pharmingen, San Diego, CA); and 6) for CXCR4, FITC-, PE-, or APC-conjugated mAb 12G5 (R & D Systems

and BD-Pharmingen), FITC-conjugated mAb 173 (R & D Systems), and unconjugated mAbs 12G5, 171, 172, and 173 (NIH AIDS Research and Reference Reagent Program). For detecting CD4, FITC- or PE-conjugated mAb Leu 3A (BD-Pharmingen) or APC- or TC (tricolor)-conjugated mAb S3.5 (Caltag Laboratories, Burlingame, CA) was used. For CD8 detection, FITC- or PE-conjugated mAb Leu 2A (BD-Pharmingen, San Diego, CA) or mAb 3B5 conjugated with APC or TC (Caltag Laboratories, Burlingame, CA) was used. In some cases, a commercial kit was used to conjugate primary antibodies with fluorescein or one of the Alexa dyes (Molecular Probes, Inc., Eugene, OR). For secondary staining, dye-conjugated purified Fab fragments with the relevant species specific reactivity were obtained from commercial sources (Molecular Probes and Jackson Immunoresearch Laboratories, West Grove, PA).

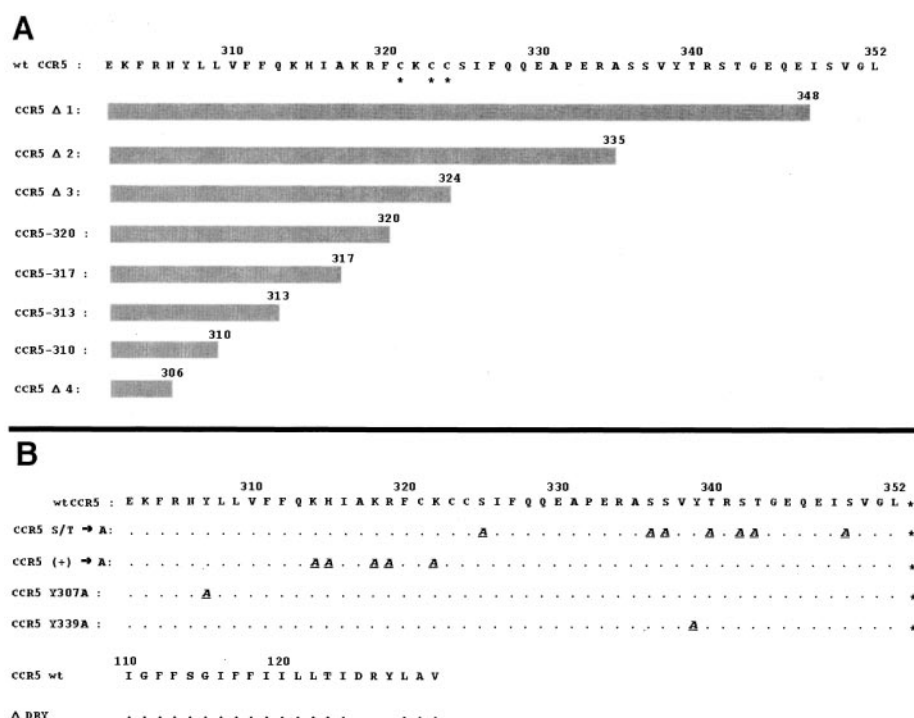
For determination of cell surface antibody binding, 10<sup>6</sup> cells from the respective transfections were collected by centrifugation and washed with PBS. They were incubated for 30 min at 4 °C with the respective fluorochrome-conjugated or -unconjugated monoclonal or rabbit polyclonal antibodies in 50 µl of PBS containing 3% BSA or 2% FCS and 0.02% sodium azide. The cells were washed three times with ice-cold PBS containing BSA or FCS and then resuspended in 50 µl of PBS with BSA or FCS and incubated with fluorochrome-conjugated secondary antibodies (as indicated) for 30 min at 4 °C. The cells were then washed three times with ice-cold PBS and fixed in PBS containing 4% paraformaldehyde. For detection of internal antigens, the cells were permeabilized and fixed prior to staining by use of a commercial kit (BD-Pharmingen). Flow cytometric data acquisition was by using a two-laser, four-color Becton Dickinson FACS<sup>TM</sup> flow cytometer. Data analysis was done using CELLQUEST<sup>TM</sup> version 3.3 (BD-Pharmingen) and FlowJo version 3.3.4 (The Treestar Inc., San Diego, CA) software.

**Metabolic Labeling and Immunoprecipitation**—For metabolic labeling experiments, 293-T cells (10<sup>6</sup> to 10<sup>7</sup>) at 24–30 h after transfection (as described in the appropriate figure legends) were rinsed three times with and incubated in methionine- and cysteine-free Dulbecco's modified Eagle's medium containing 2% dialyzed FCS (0.2 ml per sample) for 10 min. Cells were labeled for 1 h by the addition of <sup>35</sup>S Trans-label (ICN Biomedicals Inc., Costa Mesa, CA) to 1 mCi/ml. For measuring the kinetics of protein biosynthesis, 2 × 10<sup>7</sup> cells were labeled for 15 min in 500 µl of labeling medium (1 mCi/ml). At the end of the labeling, the cells were diluted with 10 volumes of complete RPMI medium. Aliquots were removed immediately after labeling and at the indicated periods during the chase (from 0 to 12 h). The cells were rinsed twice in PBS and processed for SDS-PAGE analysis. The cells were disrupted by three cycles of freeze-thawing in 500 µl of extraction buffer containing 0.05 M Tris-HCl, pH 7.4, 100 mM NaCl, 0.25% Nonidet P-40 (or CHAPS), 0.25% Triton X-100, and one tablet of protease inhibitor mix (Roche Molecular Biochemicals) followed by extraction at 4 °C for 1 h. The extracts were centrifuged at 15,000 × g for 10 min, and supernatants were used for immunoprecipitation.

For immunoprecipitation, supernatants were precleared by incubation for 1 h at 4 °C with 30 µl of immobilized protein G-agarose beads (Life Technologies, Inc.) coated with preimmune rabbit or mouse sera. Labeled proteins were immunoprecipitated for 3 h at 4 °C with protein G-agarose beads prebound to the corresponding anti-rabbit polyclonal or anti-mouse monoclonal antibodies. Following specific antibody binding, the immunobeads were collected by centrifugation and washed five times with 10–20 volumes of extraction buffer lacking protease inhibitors, and the labeled proteins were eluted by boiling in 50 µl of a buffer containing Tris-HCl, pH 7.4, 100 mM NaCl, 50 mM dithiothreitol, 2% SDS, glycerol (10%, v/v), and bromophenol blue (0.1%, w/v). The radio-labeled proteins were resolved by SDS-PAGE, visualized by phosphor-imaging (Molecular Dynamics, Inc., Sunnyvale, CA), and quantified.

**Confocal Immunofluorescence Microscopy**—For immunofluorescence detection of receptors on live cells, transfected cells plated on coverslips were rinsed with PBS and reacted with receptor-specific antibodies in PBS containing 0.3% BSA for 30 min at 4 °C. For CCR2B, unconjugated CCR2 mAb (R & D Systems) was used; for CCR3, FITC-conjugated rat anti-CCR3 or unconjugated rat anti-CCR3 (R & D Systems) was used; for CCR5, FITC- or APC-conjugated 2D7 (BD-Pharmingen) or FITC-conjugated 182 (R & D Systems) mAbs were used. CCR5 transfections were also checked with rabbit serum against N-terminal peptide of CCR5. CDw168 and IL8-Rb mAbs (BD-Pharmingen, San Diego, CA) were used to stain for CXCR1 and CXCR2, respectively. For staining CXCR4, APC-conjugated 12G5 (BD-Pharmingen) or FITC-conjugated 12G5 or 173 (R & D Systems, Minneapolis, MN) mAbs were used. In cases where first antibodies were unlabeled, the coverslips were rinsed five times with PBS and stained with Alexa 488 or Texas Red-conjugated second antibodies (Fab fragments, Molecular Probes) in PBS containing 0.3% BSA for 30 min at 4 °C. After rinsing five times with

**FIG. 1. Schematic illustration of CCR5 mutants.** A, C-terminal deletions of CCR5s are denoted by the shaded rectangles ending at the designated sites. The numbered sequence of WT CCR5 is given above.  $\Delta 1$  through  $\Delta 4$  deletion mutants were tagged with a FLAG epitope at the N termini. B, sequence of WT CCR5 and of mutants that exchanged all of the serine and threonine residues for alanine (S/T  $\rightarrow$  A) or that replaced the lysines at 314, 318, and 322, arginine at 319, and histidine at 315 with alanine ((+)  $\rightarrow$  A) in the cytoplasmic tail of CCR5.  $\Delta$ DRY refers to deletion of the -DRY- motif in the second intracellular loop. Asterisks denote the three cysteines that may be palmitoylated (41).



PBS, the coverslips were mounted in Fluoromount-G (Southern Biotechnologies, Birmingham, AL). For detecting intracellular antigens, cells were fixed in 4% (v/v) paraformaldehyde for 15 min at 4 °C, rinsed five times with PBS, permeabilized by 15 min of treatment with 0.25% Triton X-100 (or Nonidet P-40) in PBS at 25 °C, and reacted as above with the respective antibody combinations.

The following organelle-specific antibodies were used to detect colocalization of the receptors with various subcellular compartments: 1) for ER, mAbs (Affinity Bioreagents, Golden, CO) or rabbit sera (Stressgen Biotechnologies Corp., Victoria, BC) against calnexin or calreticulin, anti-heme oxygenase mAb or rabbit anti-BiP (Stressgen Biotechnologies Corp., Victoria, Canada), or anti-protein-disulfide isomerase mAb (from Affinity Bioreagents); 2) rabbit anti- $\beta$ -COP (Sigma); 3) for Golgi, Deng mAb or mannosidase (donated by Nelson Cole of NHGRI, NIH; and Juan Bonifacio of CBMB, NICHD, NIH); 4) for TGN, anti-TGN 38 mAb (Affinity Bioreagents) or sheep anti-TGN 46 (Serotec Inc., Raleigh, NC); and 5) for plasma membrane, anti-transferrin receptor (CD71, from Beckman-Coulter, Fullerton, CA),  $\text{Na}^+/\text{K}^+$  ATPase (Affinity Bioreagents), or anti-epidermal growth factor receptor mAb (Upstate Biotechnology, Inc., Lake Placid, NY).

Images were collected on a Leica TCS-NT/SP confocal microscope (Leica Microsystems, Exton, PA) using a  $\times 63$  or  $\times 100$  oil immersion objective NA 1.32 and digital zoom up to  $\times 2.2$ . Fluorochromes were excited using an argon laser at 488 nm for Alexa 488 or FITC and a krypton laser at 568 nm for Alexa 568 or Texas Red and helium/neon laser at 633 nm for APC. Detector slits were configured to minimize any cross-talk between the channels, or the channels were collected separately and later superimposed. Differential interference contrast images were collected simultaneously with the fluorescence images using the transmitted light detector. Images were processed using the Leica TCS-NT/SP software (version 1.6.551), Imaris 3.0.2 (Bitplane AG, Zurich Switzerland), and Adobe Photoshop 6.01 (Adobe Systems, San Jose, CA).

**Intracellular  $[\text{Ca}^{2+}]$  Measurements**—Cells ( $\sim 10^7/\text{ml}$ ) were incubated in Hanks' balanced saline solution and 2.5  $\mu\text{M}$  Fura-2/AM (Molecular Probes) for 30–60 min at 37 °C in the dark. The cells were then washed with Hanks' balanced saline solution and suspended at  $10^7$  cells/ml.  $4 \times 10^6$  cells were stimulated with the indicated chemokines (purchased from Peprotech Inc., Rocky Hill, NJ) or ATP in a total volume of 2 ml in a continuously stirred cuvette at 37 °C in a fluorimeter (Photon Technology Inc., South Brunswick, NJ). Data were recorded every 200 ms as the relative ratio of fluorescence emitted at 510 nm after sequential excitation at 340 and 380 nm.

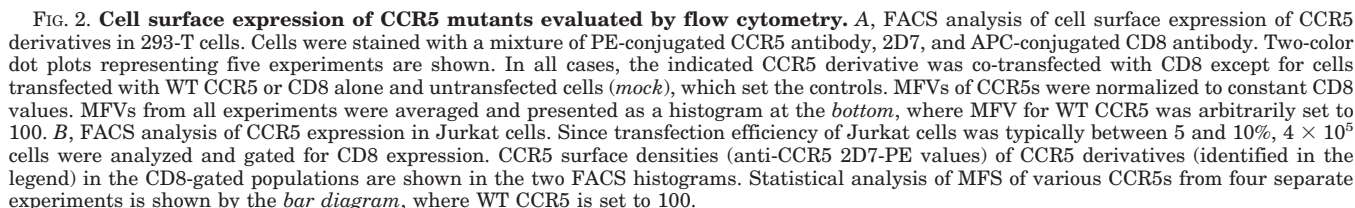
## RESULTS

**Delineation of Structural Determinants in the C-terminal Tail of CCR5 Required for Cell Surface Expression**—To identify

the carboxyl-terminal domains of CCR5 required for cell surface expression, we first engineered a C-terminal set of deletion mutants shown schematically in Fig. 1A. Deletions labeled  $\Delta 1$  through  $\Delta 4$  were also tagged at the 5'-end with a FLAG epitope, and for comparison we used a WT CCR5 carrying an identical epitope.

Steady-state cell surface expression was examined following transfection of primate epithelial cell lines including 293-T, HeLa, and COS-1 cells and Jurkat T-lymphocytes. To normalize for transfection efficiencies, CD8 was co-transfected, and the distribution of CD8 and CCR5 was examined by two-color FACS using respective monoclonal antibodies directly conjugated with nonoverlapping chromophores (*i.e.* FITC and TC or PE and APC). Representative results using 293-T cells are illustrated in Fig. 2A. Cells transfected with CD8 or WT CCR5 alone set the distinct population boundaries for cells staining positively for CCR5 or CD8. A dot plot of cells transfected with WT CCR5 and CD8 showed a double positive diagonal population with almost equivalent staining for both receptors. C-terminal truncations resulted in a progressive decrease in the relative surface density of CCR5 in the transfected populations that had equivalent CD8 expression. Mean fluorescence values (MFVs) for CCR5 were computed for the transfected population (gated for CD8) and normalized to constant CD8 values. MFVs decreased from 452 for the FLAG-WT CCR5 to 140 (a 66% reduction) for a truncation to the 320th residue. The  $\Delta 4$  mutant that lacked the entire C-tail from truncation at the 306th residue was essentially negative for surface expression in this assay. Truncation to the 320th residue lacking three cysteine residues that are targets of palmitoylation (KRFX) displayed a modest decrease when compared with the  $\Delta 3$  (KCCX) mutant of 324 residues (MFV of 110 *versus* 161 for  $\Delta 3$ ). Further truncation (HIAAX mutant) that eliminated the upstream lysine and arginine at positions 318 and 319 was severely restricted for surface expression.

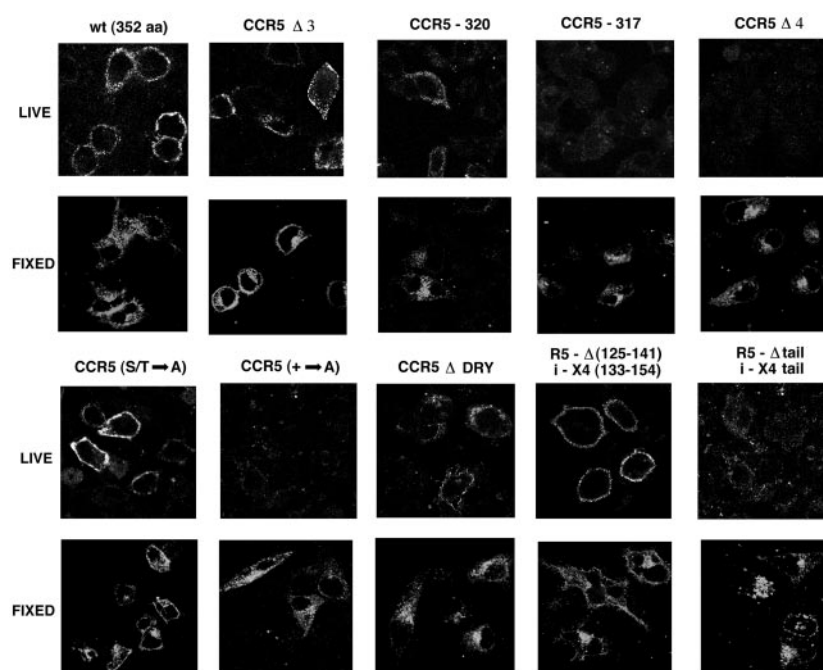
The significant drop (50–60%) from the WT expression levels for the KCCX mutant prompted us to inquire whether the serines and threonines in the C-tail, which may be targeted by GPCR kinase(s) or arrestin, are critical for surface expression. A mutant named S/T  $\rightarrow$  A, which exchanged all of the serines



Relative surface expression of all CCR5 mutants was examined in five independent experiments, and, as shown by the

histogram in Fig. 2A, they did not vary by more than 10%. Surface expression of CCR5 mutants was analyzed twice in HeLa and COS-1 cells with similar results (not shown). The expression phenotype of selected mutants was also examined in Jurkat lymphocytes. As with other cell types, truncation to the 324th residue resulted in significant decrease (~50%) in surface expression (Fig. 2B). Excision of the entire tail ( $\Delta 4$ ) eliminated surface expression. While the (+)  $\rightarrow$  A mutant was expressed, the level was significantly reduced (20–25% of WT). MFV data from four experiments in Jurkat cells are summarized by the histogram in Fig. 2B. To exclude the possibility that nonreactivity with any one antibody may have been due to altered conformations of mutant CCR5, expression of every

**FIG. 3. Confocal immunofluorescence assay of various CCR5 mutants on live and permeabilized cells.** Images were visualized by a  $\times 63$  objective of a Leica confocal microscope. For detection of CCR5s on living cells, transfected HeLa cells on 8-mm coverslips were reacted with a mixture of FITC-conjugated 2D7 and 182 antibodies. Note the decrease in the punctate surface fluorescence for the KRFX 320 aa mutant and the R5-X4 tail exchange mutant (R5  $\Delta$  tail, i-X4 tail) and the lack of surface staining for longer truncations and the (+)  $\rightarrow$  A mutant. A parallel row of coverslips were fixed and permeabilized before reaction with the same mixture of antibodies.



derivative was checked twice with seven monoclonal antibodies (2D7, 3A9, 5C7, 180, 181, 182, and 183) and once with rabbit anti-serum against the N-terminal peptide of CCR5 in 293-T transfectants. Similar expression patterns for various CCR5 mutants were observed with different antibodies (not shown). Likewise, staining with 5C7 and 3A9 antibodies and rabbit anti-CCR5 antiserum corroborated results obtained with Jurkat cells (not shown). Mutants that were negative for surface expression in HeLa and COS-1 cells with 2D7 antibody displayed the same phenotype with six different monoclonal antibodies (not shown).

**Mutants Impaired for Surface Expression Were Retained inside the Cells**—HEK 293 cells stably expressing WT or tailless CCR5 were analyzed for CCR5 antibody reactivity. When living cells were incubated with six different monoclonal antibodies, only WT CCR5 cells reacted positively; cells expressing tailless CCR5 were negative for surface staining. When the cells were fixed and permeabilized prior to antibody staining, both cell types reacted positively to three different CCR5 mAbs (not shown).

Subcellular distribution of WT and mutant CCR5 was examined by confocal immunofluorescence microscopy of live or fixed and permeabilized HeLa cells transfected with individual plasmids. Three different conjugated CCR5 monoclonal antibodies (2D7, 3A9, and 182) were used alone or in combination (2D7 and 182), and 12 fields (6–10 cells per field) were collected for each staining from two separate experiments. As shown in Fig. 3, live WT CCR5-expressing cells exhibited punctate cell surface fluorescence. C-terminal truncations reduced the surface density of CCR5 in this assay, with the H1AX mutant (317th residue) showing barely detectable surface reactivity. Both the  $\Delta 4$  (306th residue) and the (+)  $\rightarrow$  A mutant displayed very little or no surface staining. CCR5 chimeras that exchanged the CCR5 tail for that of CXCR4 (Fig. 3, R5  $\Delta$  tail, i-X4 tail) or for CCR3 tail (not shown) were also poorly visualized at the cell surface. S/T  $\rightarrow$  A mutant that exchanged all of the serines and threonines in the CCR5 tail for alanine and a mutant (R5  $\Delta$ 125–141, i-X4 (133–154)) that exchanged a 16 residues in the second ICL of CCR5 containing the -DRY- motif for a corresponding region of CXCR4 displayed WT levels of expression.  $\Delta$  DRY mutant had a somewhat reduced surface expres-

sion. There was no difference in the histological profile when transfectants were reacted with a mixture of three different unconjugated murine monoclonal antibodies or a rabbit anti-serum against CCR5 N-terminal peptide followed by staining with Alexa 488-conjugated second antibodies to maximize detection of poor surface expressers (not shown). When transfectants expressing the CCR5 mutants were fixed and permeabilized prior to antibody staining, all of the CCR5 derivatives displayed similar levels of intracellular antibody reactivity (Fig. 3).

**Intracellular Signaling and HIV Usage Were Impaired for CCR5 Mutants Defective for Surface Expression**— $\text{Ca}^{2+}$  flux analysis was done with 293-T cells co-transfected with CD8 and selected CCR5 plasmids.  $10^6$  cell aliquots of indicated transfectants were labeled with [ $^{35}\text{S}$ ]methionine, and the cell extracts were immunoprecipitated with rabbit anti-CCR5 antiserum. Immunoprecipitates were resolved by SDS-PAGE and visualized by PhosphorImager scanning. The various CCR5 derivatives were expressed as well if not better than WT CCR5 (Fig. 4). Cells were analyzed for CD8 expression, and the individual transfectants were adjusted to constant CD8+ levels. Approximately  $5 \times 10^6$  cells were preloaded with Fura-2 and analyzed for intracellular  $\text{Ca}^{2+}$  flux following sequential additions of 100 nM RANTES and ATP. Appending FLAG or HA epitopes at the N or C terminus or His<sub>6</sub> tag at the C terminus of CCR5s did not impair the signaling potential of the resulting tagged CCR5s (not shown). Distal deletions up to the 324th residue were competent for signaling, while the tailless CCR5,  $\Delta 4$ , was negative in this assay (Fig. 4). With cells expressing the (+)  $\rightarrow$  A mutant, there was a barely detectable hump rather than a spike of  $\text{Ca}^{2+}$  flux, and the  $\Delta$ DRY mutant that lacked the G-protein binding motif was silent as expected. Examining the ligand-dependent CCR5 phosphorylation validated these findings; mutants that were negative for surface FACS expression or  $\text{Ca}^{2+}$  flux displayed no phosphorylation.<sup>2</sup>

CCR5 expression levels influence the magnitude of HIV infection, and the tailless CCR5 has been shown to facilitate M-tropic HIV env-induced fusion *in vitro* (36–38). We exam-

<sup>2</sup> D. I. Van Ryk and S. Venkatesan, unpublished data.

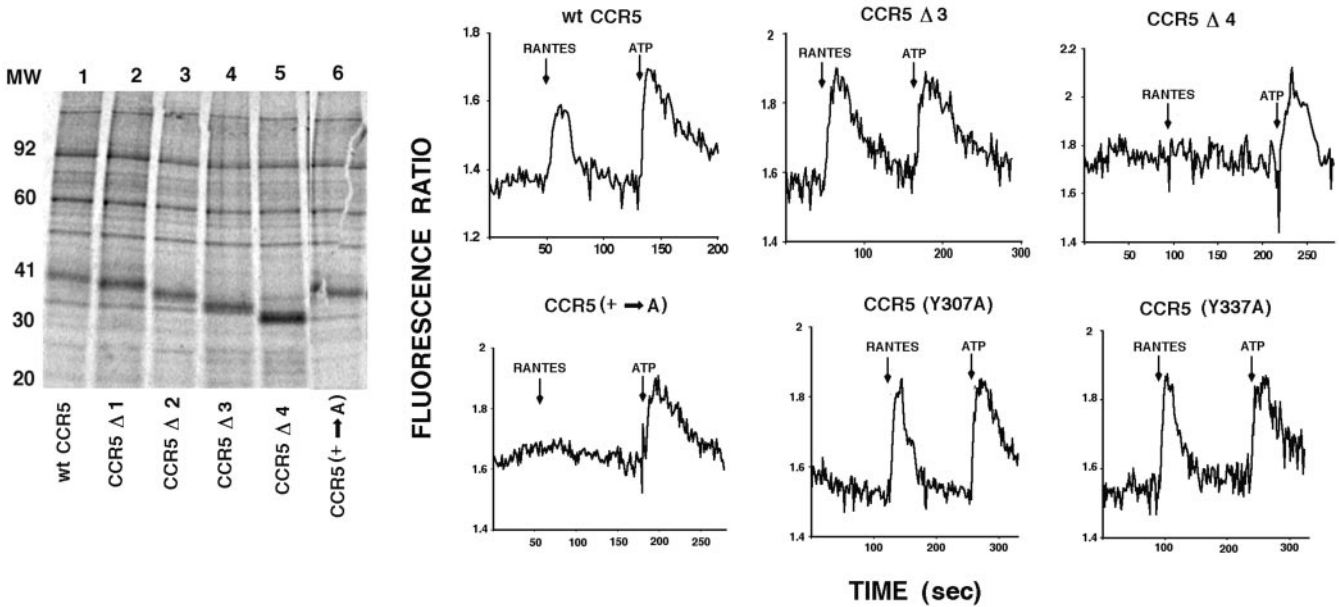


FIG. 4. **Detection of *de novo* synthesized CCR5 mutants and measurement of their signaling potential in response to chemokine stimulation.** An aliquot ( $10^6$  cells) of transfected cells was metabolically labeled and processed for immunoprecipitation using rabbit antiserum against the N-terminal CCR5 peptide. A fluorogram of the SDS-PAGE profile is shown on the *left*. Intracellular  $\text{Ca}^{2+}$  signaling of 293-T cells transfected with the respective CCR5 derivatives is shown on the *right*. Relative fluorimetric ratios are plotted as a function of time. The *arrows* denote times of the addition of RANTES or ATP ligands.

ined M-tropic virus entry more directly using a luciferase-expressing virus pseudotyped with the M-tropic envelope, JRFL. 293T cells were transfected with CD4 or with equimolar mixtures of CD4 and WT or  $\Delta 4$  CCR5. CD4+ cells were purified by magnetic bead technology and infected with luciferase-expressing NL-432 HIV pseudotyped with JRFL or amphotropic murine leukemia virus envelope protein and assayed for luciferase expression. Luciferase expression in each case was normalized to constant levels of CD4 expression as described under "Materials and Methods." In three independent experiments, HIV entry into the  $\Delta 4$  cells was at least 7% as efficient as the WT cells (Table I). This was comparable with the nearly 95% reduction in the surface expression of CCR5 observed with the  $\Delta 4$  CCR5 by FACS analysis. HIV usage of (+)  $\rightarrow$  A mutants was impaired by a similar magnitude (not shown).

**C-terminal Domain of CXCR4 Failed to Rescue the Trafficking Defect of Tailless CCR5**—To investigate whether the anterograde transport of CCR5 required a specific CCR5 C-terminal domain or whether tails of other chemokine receptors would suffice, we generated a chimera substituting the C-terminal domain of CXCR4 for that of CCR5. The R5-X4 (R5  $\Delta$  tail (296–352)-i-X4 tail (301–352)) chimera displayed poor or no surface expression, behaving like the tailless  $\Delta 4$  CCR5 (Fig. 5A). Live cell microscopy showed that this chimera had strongly reduced surface expression (Fig. 3). In contrast, substitution of the second extracellular loop of CXCR4 containing the -DRY- motif for that of CCR5 displayed an almost WT phenotype for surface expression by FACS analysis (Fig. 5A) or immunofluorescence microscopy (Fig. 3), and RANTES was able to activate this chimera and induce calcium flux (not shown).

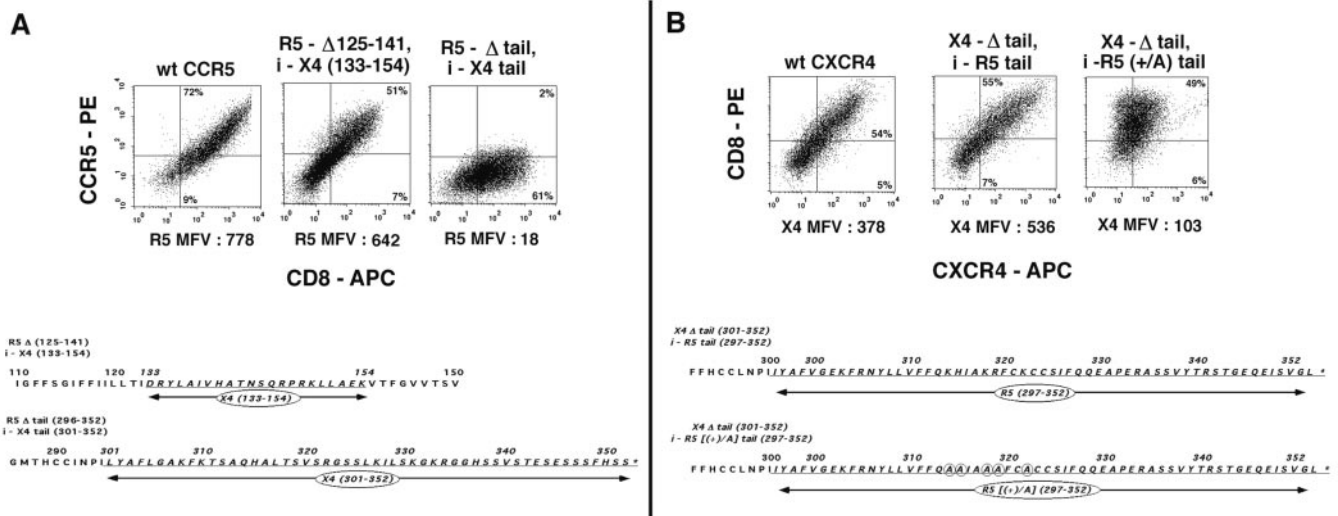
In contrast to CCR5, deletion of the cytoplasmic domain had no effect on the surface expression of CXCR4 (not shown), consistent with previous reports. Exchange of the CXCR4 tail for that of CCR5 (X4  $\Delta$  tail (301–352)-i-R5 tail (296–352)) also did not reduce the surface expression of the resulting X4-R5 chimera by FACS analysis. Live cell immunofluorescence assay of transfectants expressing the LGAX truncation mutant or the

TABLE I  
*Luciferase assay results represent the average of three measurements and are expressed in arbitrary machine units (see "Materials and Methods"). NO, background values when no virus was used; JRFL, M-tropic HIV; AMLV, amphotropic murine leukemia virus. Expt., experiment.*

	NO	JRFL	AMLV
Expt. 1			
CD4 only	17	26	6750
CD4 + WT CCR5	58	3900	8700
CD4 + CCR5 $\Delta 4$	78	314	7200
Expt. 2			
CD4 only	81	13	9700
CD4 + WT CCR5	78	2800	8200
CD4 + CCR5 $\Delta 4$	52	188	8900
Expt. 3			
CD4 only	44	88	8100
CD4 + WT CCR5	58	4100	7300
CD4 + CCR5 $\Delta 4$	78	286	6800

X4-R5 chimera confirmed their unaltered surface expression potential (Fig. 10). When the CCR5 cytoplasmic domain in the X4-R5 chimera was from the (+)  $\rightarrow$  A CCR5 mutant that changed the three lysines at 314, 318, and 322, histidine at 315, and arginine at 319 to alanine(s), cell surface expression of the resulting chimera (X4  $\Delta$  tail (301–352)-i- R5[(+)A] tail (296–352)) was somewhat reduced. Fig. 5B represents the maximal reduction in the cell surface expression of CXCR4 reactivity observed with this chimera.

**Cell Surface Expression of Certain C-C and CXC Chemokine Receptors Also Required Variable Lengths of Cytoplasmic Tail**—Next, we inquired whether other chemokine receptors require a complete cytoplasmic tail for cell surface expression. For this purpose, we chose CCR2B and CCR3, two C-C chemokine receptors closely related to CCR5, and two CXC chemokine receptors, CXCR1 and CXCR2, which are related to CXCR4. The cytoplasmic tails of these receptors were truncated to different lengths as shown by the *scheme* in Fig. 6A. Cell surface expression of the respective WT and mutant receptors was evaluated by two-color FACS in 293-T transfectants. CD8+ cells were gated and evaluated for co-expression of



**FIG. 5. Cell surface expression of CCR5 and CXCR4 chimeras.** A, FACS analysis of cell surface expression of CCR5 mutants that exchanged the second ICL containing the -DRY- motif for that of CXCR4 and mutants that transposed the C-terminal cytoplasmic domain for that of CXCR4. Two-color dot plots representing three experiments using 293-T cells are shown as in Fig. 2A. CCR5 mutants are identified at the top of each plot. MFVs of CCR5s were normalized to constant CD8 values. Primary structure and the sequence coordinates of the chimeras are given below the plots. B, cell surface expression of CXCR4 mutants with exchanges of the cytoplasmic domain. 293-T transfectants were stained with a mixture of APC-conjugated CXCR4 antibody, 12G5, and PE-conjugated CD8 antibody. Two-color dot plots representing three separate experiments are similar to A, except that CXCR4-APC is on the *abscissa* and CD8-PE on the *ordinate*. Photomultiplier gain was adjusted to minimize the MFV for the endogenous CXCR4 in 293-T cells to <30. MFVs for CXCR4 were normalized to CD8 expression. The sequence of the mutants is given below the plots.

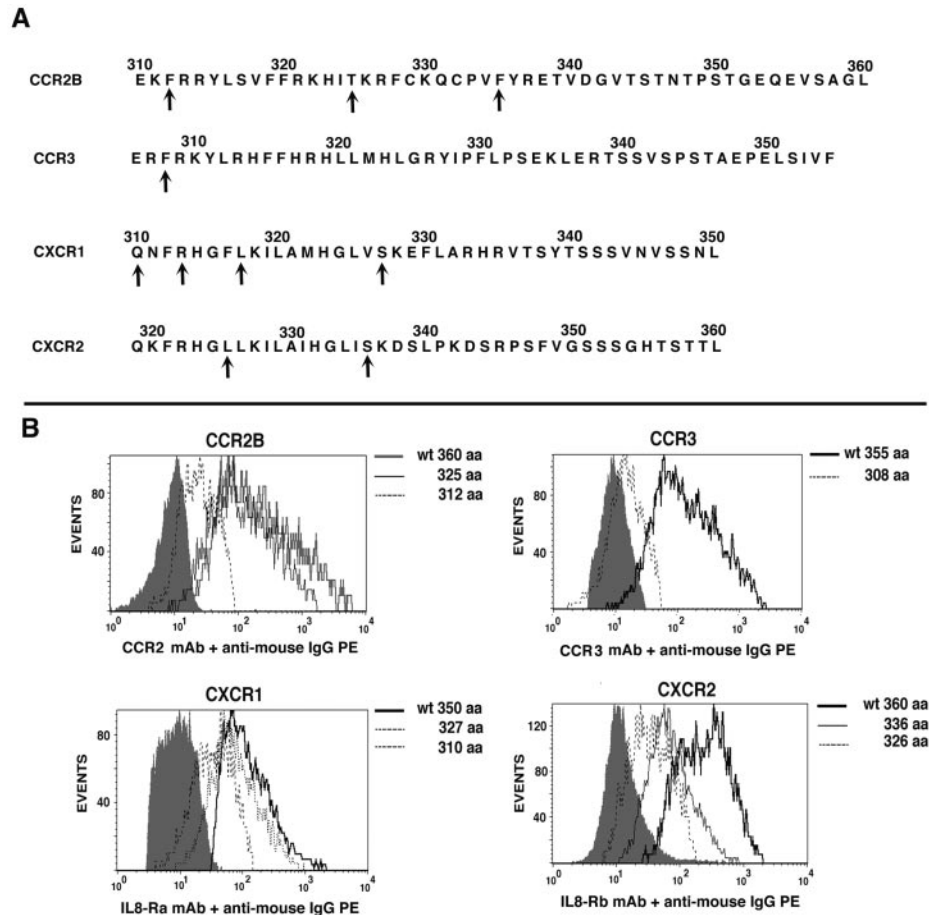
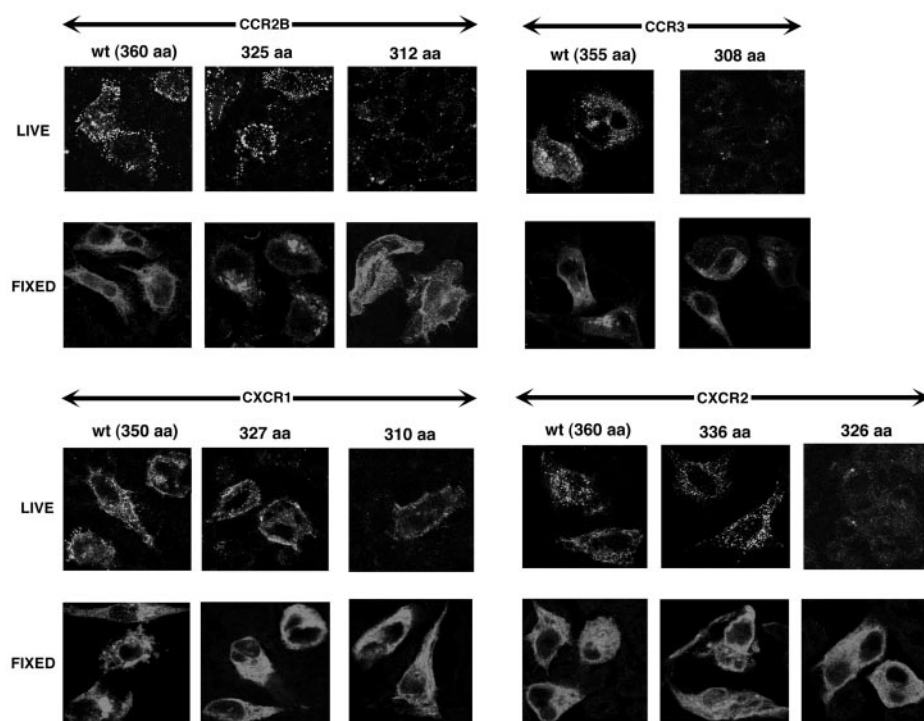


**FIG. 6. Sequence requirements for cell surface expression of various CC and CXC chemokine receptors.** A, primary structure of cytoplasmic domain of CC and CXC receptors used in this study. The arrows denote the C termini of various deletion mutants described throughout. B, FACS analysis of expression of WT and selected mutants of CCR2B, CCR3, CXCR1, and CXCR2 chemokine receptors. 293-T cells were co-transfected with CD8 and the indicated WT or mutant receptor and analyzed for surface expression with a mixture of CCR3-PE and CD8-APC for CCR3 transfectants; CXCR2-PE and CD8-APC for CXCR2 expressors; CCR2 mAb followed by PE conjugated anti-mouse IgG followed by CD8-APC for CCR2B transfectants; and CDw128 mAb followed by PE-conjugated anti-mouse IgG followed by CD8-APC for CXCR1 cells. Cells gated for CD8 reactivity were analyzed for reactivity with the respective chemokine receptor antibodies. Cells transfected with CD8 alone were reacted with the respective chemokine receptor antibodies and served as the negative controls (*shaded graphs*). FACS profiles of three representative experiments are shown.

the respective chemokine receptors. Substantial truncation of the CCR2B tail (Fig. 6B, Δ1, 325 aa) had very little effect on cell surface expression. Further trimming of the C terminus of CCR2B (Δ2, 312 aa) that removed a portion of the seventh TM domain did not entirely abrogate surface expression but re-

duced it by 5-fold. Excision of most of the C-terminal domain of CCR3 drastically reduced, if not abolished, the cell surface expression as shown by the FACS profile in Fig. 6B. In contrast, removal of the entire C-terminal tail of CXCR1 resulted only in a modest reduction in the surface expression of the

**FIG. 7. Confocal immunofluorescence assay of CCR2B, CCR3, CXCR1, and CXCR2 receptor expression on live and permeabilized cells.** Conditions are similar to those described for Fig. 3 except for the use of the following monoclonal antibodies: unconjugated CCR2 antibody (clone 48607) followed by Alexa 488-conjugated anti-mouse IgG; FITC-conjugated rat antibody (clone 61828) against CCR3; FITC-conjugated antibody (clone 42705) against CXCR1 or unconjugated anti-CXCR1 antibody (anti-CDw128) followed by Alexa 488-conjugated anti-mouse IgG; and FITC-conjugated antibody (clone 48311) against CXCR2 or unconjugated anti-CXCR2 antibody (anti-IL-8 Rb) followed by Alexa 488-conjugated anti-mouse IgG.



receptor (Fig. 6B). In comparison, C-terminal truncations of CXCR2 resulted in more significant reduction in trafficking to the cell surface than corresponding CXCR1 mutants (Fig. 6B). Although CXCR1 and CXCR2 mutants were expressed better at the cell surface than the CCR2B, CCR3, and CCR5 counterparts, although at reduced levels, surface expression of tailless CXCR4 was not affected. The above results were confirmed by transfections of HeLa and COS-1 cells (not shown).

The cell surface expression pattern obtained by FACS analysis was validated by immunofluorescence microscopy of living or fixed and permeabilized HeLa cells transfected with the respective receptor plasmids (Fig. 7). As expected, there was no difference in the magnitude of intracellular antibody reactivity of the various mutants. Surface fluorescence was undiminished for the CCR2B mutant truncated at the 325th amino acid but was markedly reduced for the mutant truncated at the 312th residue, much more than was anticipated by FACS data. The CCR3 mutant lacking the C-tail was poorly expressed on the living cells. Excision of CXCR1 C-tail did not curtail surface expression on living cells (Fig. 7, WT *versus* 310 aa), while equivalent C-terminal truncations of CXCR2 led to progressive decrease in expression on living cells (Fig. 7, WT *versus* 336 and 326 aa).

**C-terminal Truncations of CCR5 Showed No Obvious Defects in Turnover**—To test whether C-terminal truncation of CCR5 affected intracellular turnover in addition to trafficking, we carried out metabolic labeling experiments. For this purpose 293-T cells were co-transfected with CD8 and the indicated CCR5 plasmid. Pulse-chase analysis of protein synthesis was as described under "Materials and Methods." Individual time points were evaluated for CD8 expression, and the aliquots from various transfectants were adjusted to constant CD8 expression. CCR5 was immunoprecipitated using a rabbit antiserum raised against the N-terminal peptide of CCR5. Quantitative recovery of CCR5 was more consistently obtained with the rabbit antiserum than with monoclonal antibodies against CCR5 or FLAG epitope. The SDS-PAGE profile of individual labeling kinetics shown in Fig. 8 is representative of three experiments. Nascent WT CCR5 was rapidly converted to a

slowly migrating species within 1 h of chase. In accordance with an earlier report (46), this species probably reflected the *O*-glycosylated form of CCR5. There was no obvious difference in the rates of turnover of WT or various C-terminal truncations, with the calculated  $t_{1/2}$  durations in the range of 6–9 h. C-terminal truncation of CCR5 resulted in progressive loss in the intensity of *O*-glycosylated species, with the  $\Delta 2$  mutant that is well expressed at the cell surface showing very little *O*-glycosylation.

**Transport-defective CCR5 Mutants Were Retained in the ER / Golgi Compartments**—The subcellular distribution of CCR5 mutants was examined by confocal microscopy of fixed and permeabilized transfectants immunostained with a mixture of antibodies against CCR5 and the indicated organelle component(s). Due to overexpression, WT and each mutant accumulated in the ER. To facilitate clearing of nascent proteins from the ER, cells were briefly treated with cycloheximide prior to harvesting. With CCR5 pseudocolored in *green* and the organelles in *red*, co-localized regions appear *yellow* (Fig. 9). Co-localization was authenticated by confirming that at least five successive 0.25  $\mu$  confocal planes displayed a similar intensity of co-staining. WT CCR5 was mostly distributed at or near the periphery of the cells, co-localizing with plasma membrane markers such as transferrin receptor (Fig. 9),  $\text{Na}^+/\text{K}^+$  ATPase, or epidermal growth factor receptor (not shown). The KRFX mutant of 320 aa that had reduced cell surface expression was also distributed at the periphery of the cell. However, this mutant exhibited less uniform co-staining (note the patchy *yellow* regions) than the WT receptor with the authentic plasma membrane marker. The tailless  $\Delta 4$  mutant of 306 residues and the (+)  $\rightarrow$  A mutant with changes at the basic residues in the tail were not visualized at the plasma membrane. Although the  $\Delta 4$  mutant displayed an ER-like staining pattern, it did not co-stain with the indicated ER marker to any significant extent, judging by the clear separation of colors. Other ER markers such as antibodies against calnexin or heme oxygenase also did not show significant co-staining with  $\Delta 4$  mutant (not shown).

To test whether the mutants were retained in the vesicular

**FIG. 8. Kinetic analysis of metabolic turnover of CCR5 derivatives.** 293-T cells (two six-well plates for each) were co-transfected with CD8 and the indicated CCR5 plasmids. FACS was used to monitor transfectants for CD8 and CCR5 expression. Cells were labeled for 15 min with [ $^{35}$ S]methionine and chased with unlabeled amino acid mix for the indicated times. One-third aliquot from each time point was analyzed for CD8 labeling by SDS-PAGE and PhosphorImager scanning. CD8 turned over with a  $t_{1/2}$  of 10–12 h. The remaining aliquots were adjusted to reflect constant CD8 levels for the respective time points, and CCR5 was immunoprecipitated and processed for SDS-PAGE. Scanned images of SDS-PAGE are shown. Chase times are shown *above* each gel. Lane *M* shows molecular mass markers with the respective masses in kDa on the left. An asterisk denotes the *O*-glycosylated CCR5 band.

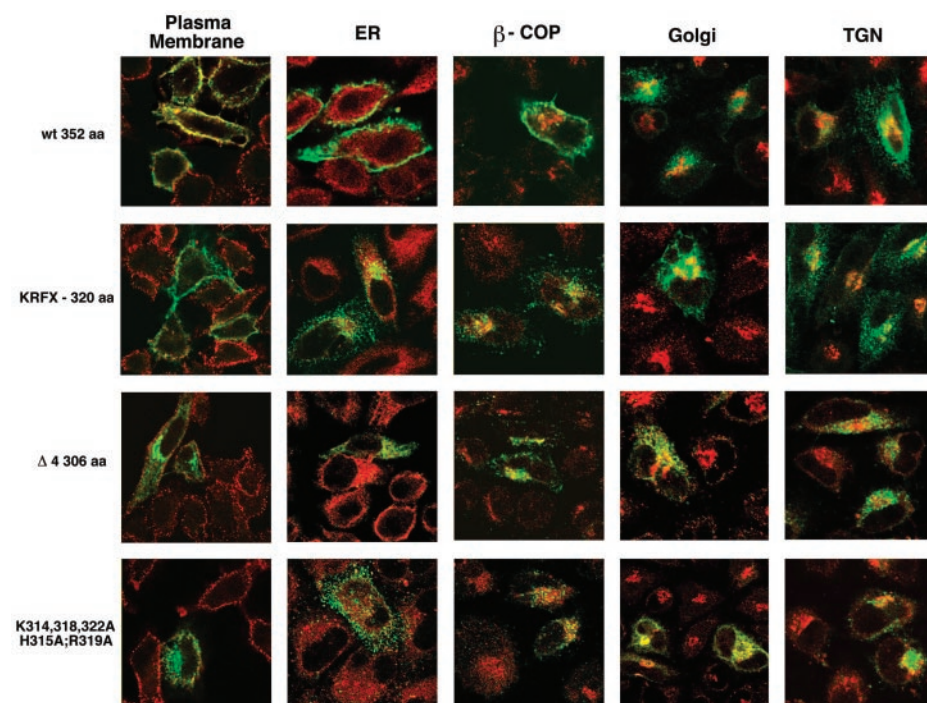
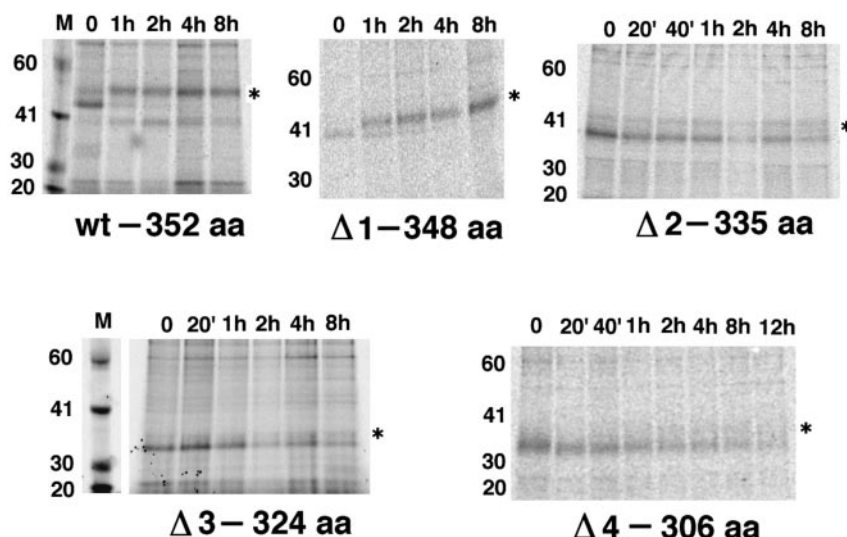


**FIG. 9. Subcellular distributions of CCR5 derivatives.** HeLa cells transfected with the indicated CCR5 plasmids were treated with cycloheximide for 30 min prior to fixation and detergent treatment. Antibody staining and confocal microscopy are described under "Materials and Methods." For co-staining plasma membrane and CCR5, a mixture of FITC-conjugated CD71 and APC-conjugated 2D7 was used. Golgi was stained with Deng antibody followed by TRITC-conjugated anti-mouse IgM and counterstained with a mixture of FITC-conjugated CCR5 antibodies 2D7 and 182. ER was stained with rabbit anti-calreticulin,  $\beta$ -COP was stained with rabbit anti- $\beta$ -COP, and TGN was stained with sheep anti-TGN 46, followed by second staining with Alexa 488-conjugated anti-rabbit or sheep IgGs. Samples were then counterstained for CCR5 with APC-conjugated 2D7. CCR5 is colored *green*, and the organelle in *red*.

compartments of anterograde transport, the cells were co-stained for CCR5 and  $\beta$ -COP (for transport vesicles between the ER and the Golgi), Golgi-resident proteins (Deng or mannosidase), or TGN 46, respectively. WT CCR5 showed little if any co-localization with  $\beta$ -COP organelles or cis and medial Golgi vesicles. There was some co-staining with the TGN vesicles, probably representing sequestration in the recycling compartment. The KRFX mutant that had reduced surface expression exhibited comparatively more co-localization with the Golgi and the TGN compartments. The  $\Delta 4$  and (+)  $\rightarrow$  A mutants that were not transported to the cell surface displayed more pronounced localization in the proximal  $\beta$ -COP vesicles and more distal Golgi compartments. HEK-293 cells stably expressing the  $\Delta 4$  mutant also displayed localization of mutant CCR5 in the ER and the Golgi compartment (not shown). The R5-X4 chimera that exchanged the CCR5 tail for that of CXCR4 and was negative for surface expression by FACS analysis (Fig. 5) was retained in the ER and Golgi compartments (not shown).

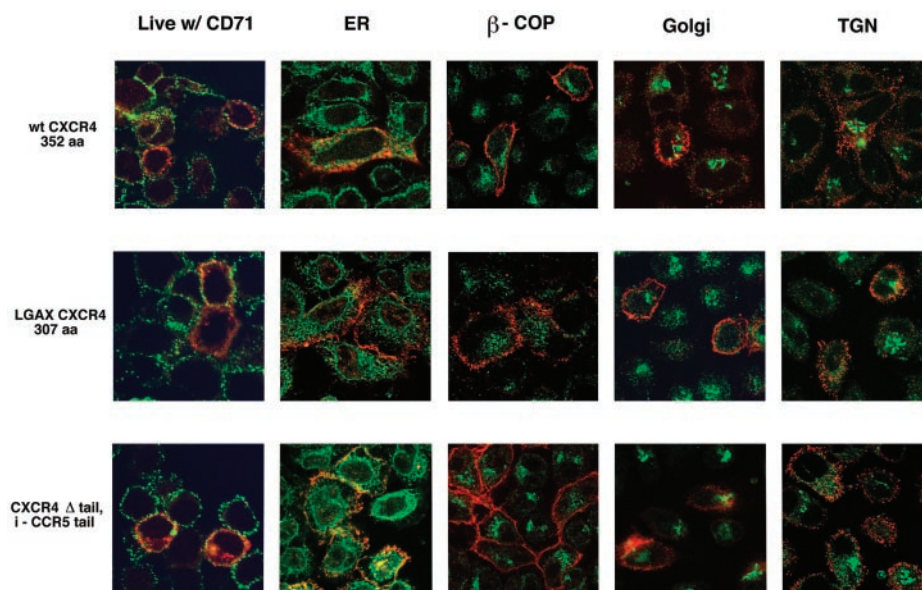
**Tailless CXCR4 and a CXCR4 Chimera with the C-tail of WT CCR5 Were Not Retained inside Cells**—We examined the sub-

cellular distribution of CXCR4 and its derivatives in transfected HeLa cells by co-staining for the receptor and cellular organelles (Fig. 5). Since CXCR4 is expressed in this and most other cell types, confocal images were collected at low laser power to minimize the contribution from the endogenous receptor. WT CXCR4 was identified predominantly at the plasma membrane of transfected cells after a brief cycloheximide treatment. This resembled the surface distribution of CXCR4 when live cells were stained (Fig. 10). There was very little if any stasis of CXCR4 in the ER or Golgi or TGN vesicles. The tailless CXCR4 mutant, LGAX, and the X4-R5 chimera that transposed the CXCR4 tail for that of CCR5 displayed a similar distribution. These CXCR4 mutants and WT CXCR4 displayed no trafficking defects in HOS cell lines selected for stable expression of these receptors (not shown).

#### DISCUSSION

In this paper, we have defined the structural requirements in the C-tail for cell surface expression of CCR5. Optimal surface expression of CCR5 is dependent on 1) the length of the

**FIG. 10. Subcellular distributions of CXCR4 derivatives.** Experimental conditions are similar to those described for Fig. 9 except for the use of APC-conjugated anti-CXCR4 antibody 12G5 instead of CCR5 antibody. Panels labeled *Live w/CD71* represent staining of living cells with a mixture of FITC-conjugated CD71 and APC-conjugated 12G5. CXCR4 is colored *red*, and the organelles are *green*.



C-tail, 2) a membrane-proximal basic amino acid-rich domain, and 3) a cysteine cluster. These sequence features act cooperatively to facilitate plasma membrane insertion of CCR5. Sequential truncations of the cytoplasmic tail caused progressive decrease in the trafficking of the receptor to the cell surface, and complete removal of the tail ( $\Delta 4$  mutant) almost totally abolished trafficking to the cell surface. The same phenotype was observed for WT and tailless CCR5 in both transfected cell lines and transiently transfected epithelial and Jurkat T cells. Although the  $\Delta 4$  mutant was not detectable at the cell surface by FACS or by ligand-induced  $\text{Ca}^{2+}$  flux, it did support low levels of M-tropic HIV entry, indicating that there must have been some surface expression. A previous report showing that the  $\Delta 4$  mutant could be expressed in NIH 3T3 cells and support M-tropic HIV infection probably reflected this residual surface expression amplified by the vaccinia vector system (38).

Exchanging the native CCR5 cytoplasmic domain for that of CXCR4 impaired the surface expression of the CCR5 chimera, indicating that a specific tail sequence and not any sequence of a particular length is required. Loss of surface expression of CCR5 deletions or tail exchanges was paralleled by enhanced intracellular retention. Alanine scanning mutagenesis of the tyrosine or serine and threonine residues in the cytoplasmic domain did not impair surface expression of CCR5, excluding role(s) for receptor phosphorylation by tyrosine kinases or Ser/Thr (GPCR-linked, protein kinase C, or other) kinases in receptor transport. Changes at the serine residues (S/T  $\rightarrow$  A mutant) increased the steady state levels of CCR5, and cells expressing this mutant gave a protracted intracellular  $\text{Ca}^{2+}$  flux response to  $\beta$ -chemokines (not shown), probably reflecting a block in receptor internalization.

CCR5 has closest sequence homology with CCR2B, followed by CCR3. It was notable that truncations of the CCR2B C-tail did not result in a comparable trafficking defect. Interestingly, truncation to the 326th residue excised both the basic domain and the cysteine cluster in the CCR2B C-tail but did not affect surface expression. These findings are consistent with an earlier report showing that truncations of CCR2B up to the 316th position did not impair surface expression (16). Further, we have shown that excision of the entire C-tail and a few residues in the upstream seventh TM domain of CCR2B (mutant 312 aa) severely reduced, but did not abolish, surface expression. Like-

wise, excision of the CCR3 C-tail (mutant 308 aa) caused severe reduction in surface expression without abolishing it. In contrast, cell surface expression of CXC chemokine receptors showed much less reliance on the presence of a C-tail. CXCR4, whose expression was unaffected by excision of the C-tail, was notable in this regard, in agreement with earlier reports (20–23) of mutants truncated to the 316th position in the C-tail (equivalent to our ALTX mutant). Serial truncations of CXCR2 have been shown to result in a progressive loss of surface expression, and the cells expressing the tailless receptor failed to be chemoattracted by IL-8 (17, 18). Similarly, we observed that C-tail truncations of CXCR2 led to progressive loss of surface expression. We have further extended this by showing that expression of CXCR1 was more resistant to C-tail truncation than CXCR2.

Those mutants that expressed poorly at the cell surface appeared to fold properly, since they reacted normally with antibodies directed against conformational or linear epitopes. We considered the possibility that the reduced surface expression was due to an increased rate of endocytosis rather than defective anterograde transport. However, preincubation of cells expressing the tailless  $\Delta 4$  mutant at 0–4 °C in the presence of  $\text{NaN}_3$ , 2-deoxyglucose, and NaF, agents that retard endocytosis rates, failed to enhance the steady-state levels of cell surface CCR5, ruling out this mechanism. It is possible that the mutants we have described may have altered ligand binding affinities in addition to impaired surface presentation. However, it was previously shown that the complete truncation of the C-terminal tail of CCR5 did not affect this parameter (38). It is highly unlikely that the other mutations considered in the present paper, all of which perturb CCR5 structure to a lesser degree, would affect ligand binding.

Many secretory and membrane-bound glycoproteins are scanned by the ER quality control system, and aberrantly folded proteins are targeted for degradation in the ER or the cytosol (47–49). Among GPCRs, inefficient processing of  $\delta$  opioid receptor results in substantial ER retention of *de novo* synthesized receptor (50) that is translocated to the cytosol, deglycosylated, ubiquitinated, and degraded by the proteasome (51). In addition,  $\beta_2$ -adrenergic receptor expression in HEK-293 cells is augmented by proteasome inhibition (52), and rhodopsin undergoes ubiquitination (53). In contrast to the above, CCR5 truncation mutants that were reduced or absent at the

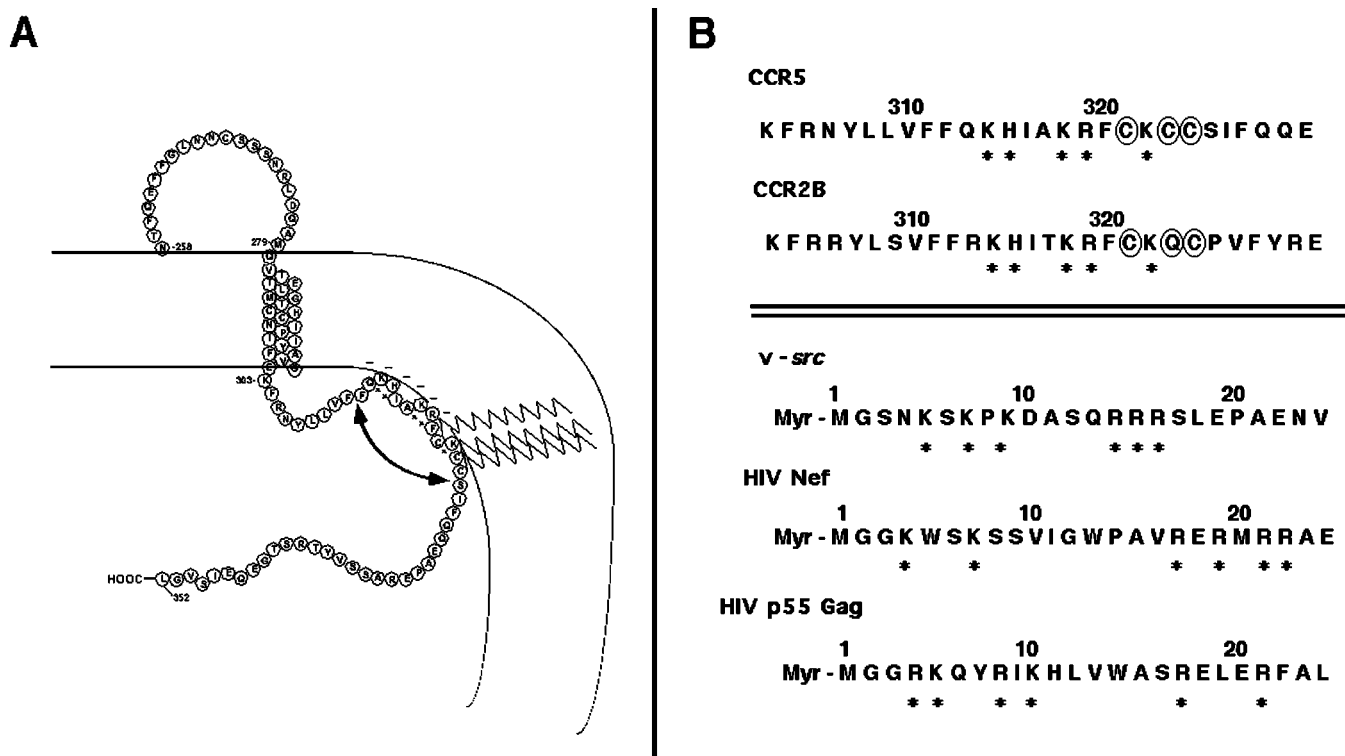


FIG. 11. Schematic diagram of a model depicting the potential membrane anchoring role(s) of the bipartite motif in the C-tail of CCR5. A, line drawing of secondary structure of CCR5 limited to the third extracellular loop, seventh TM domain, and C-terminal tail with the amino acid residues denoted by single letter codes. An arc with arrowheads highlights the bipartite motif including the membrane-proximal basic domain and the cysteine cluster. The zigzag lines represent one or more cysteines that are candidates to be potential targets for palmitoylation. B, relevant membrane-proximal regions of CCR5 and CCR2B C-tails are shown with the basic residues and the cysteine cluster denoted by asterisks and ovals, respectively. N-terminal domains of selected myristoylated proteins whose membrane anchorage is facilitated by N-terminal basic amino acids are shown.

cell surface did not exhibit significant differences in metabolic turnover compared with the WT receptor. Taken together, these observations suggest that defect(s) in anterograde transport may be the mechanism underlying impaired surface expression of CCR5 mutants.

We found that even the shortest deletions that were only slightly reduced on the cell surface had less *O*-glycosylation, unlike the WT receptor that was almost fully glycosylated within 1 h after labeling. The initial *O*-glycan addition to proteins is presumed to occur in the Golgi, with terminal modification(s) occurring in the distal Golgi stacks and sialylation in the TGN (54–60). Reduced *O*-glycosylation of mutants that were only slightly reduced at the cell surface may simply reflect their sluggish vesicular transport. Alternatively, the mutants may not have been fully glycosylated or sialylated. These findings were consistent with the co-localization patterns of various CCR5 mutants with subcellular organelles. Whereas WT CCR5 was predominantly distributed at the plasma membrane, the expression-defective mutants exhibited increasing stasis in the Golgi and the TGN compartments, and the tailless CCR5 displayed ER-like staining but co-localized with the Golgi and TGN markers.

Although the precise mechanisms underlying impaired transport and intracellular retention of CCR5 mutants are not known, they may be analogous to those that have been proposed for the retention of Golgi-resident proteins (61–64) and coronavirus glycoproteins (65–67). A “kin recognition” model (62) proposed that Golgi proteins form large oligomers mediated by their membrane-spanning domains precluding further transport. An alternative proposal suggested that cholesterol-enriched plasma membrane, being “thicker” than Golgi membranes, allowed Golgi retention of proteins with shorter and

less hydrophobic TM domains that might be sorted away from the thicker plasma membranes (61, 68, 69). The defective phenotype of CCR5 mutants may reflect one or both of these scenarios. Trafficking problems resulting from C-terminal truncations were not confined to CCR5. Excision of the entire C-terminal domains of two other CC chemokine receptors, CCR2B and CCR3, also resulted in severe reduction of surface expression and increased retention in the ER/Golgi compartments (not shown). These observations imply that cytoplasmic retention of the various tailless receptors reflects intrinsic differences in the oligomerization potential of the respective TM domains that may trap them in the Golgi apparatus. Cytoplasmic domain(s) of CCR5, CCR3, and CCR2B may then be thought of as positive regulator(s) of anterograde transport that prevent retention by facilitating rapid transit through the Golgi by interacting with putative cellular escorts. Failure of the cytoplasmic domain of CXCR4 to rescue expression for tailless CCR5 implies that the potential interactions with cellular factors may be highly specific.

Naturally occurring mutants in certain GPCRs identified in specific inherited diseases such as rhodopsin mutants in retinitis pigmentosa (70), LH receptor mutants in male pseudohermaphroditism (71), and V2-vasopressin mutants associated with congenital diabetes insipidus (72) display poor surface expression and ER retention. Some of these mutants, like the rhodopsin Q344ter mutant (73) and vasopressin V2 receptor mutant in the -ELRSLCC- domain (74), map to the C-tail of the respective receptors. This has led to a search to identify specific cellular chaperones that may be recruited to facilitate proper folding of GPCRs. Maturation of rhodopsin in the photoreceptor cells of *Drosophila* and of bovine rhodopsin is facilitated by a cyclophilin-like chaperone (75–78). Similar helper

systems have been proposed for the maturation of olfactory (79), adrenomedullin (80) receptors. In the case of  $\gamma$ -aminobutyric acid type B-1 receptors, heterodimerization with the  $\gamma$ -aminobutyric acid B-2 subunit facilitates functional surface expression (81). Some of these mechanisms may be relevant to chemokine receptors. The CCR2A isoform of CCR2, which has significant homology with CCR5, is a case in point. CCR2A, whose cytoplasmic domain is distinct from other chemokine receptors, is retained mostly in the cytosol, while CCR2B is transported efficiently to the cell surface (15). C-terminal deletions of CCR2A identified a putative retention signal in the C-tail, since the surface expression of C-terminally truncated CCR2A approached the levels of the CCR2B isoform (15). It is pertinent to note in this regard that two membrane-distal motifs, termed *is1* and *is2*, have been identified in the C-tail of HIV-1 TM glycoprotein, gp41, that cause Golgi retention of gp41 and chimeric proteins carrying these motifs (82). CCR2A C-tail sequence displayed significant homology with the *is2* element in the C-tail of gp41.

CCR5 has a cluster of three cysteines in the C-tail that are targets for palmitoylation and crucial for optimal surface expression (41). The cysteine cluster is immediately downstream of the basic residues mutated in the expression-negative (+)  $\rightarrow$  A mutant. Surface expression for the 320-residue KRFX mutant that lacks palmitoylation was significantly lower than for the 324-residue  $\Delta 3$  (KCCX) mutants. But the loss of palmitoylation sites in the KRFX mutant did not abolish functional surface expression. In contrast, alanine substitution at the membrane-proximal basic domain in the (+)  $\rightarrow$  A mutant was inhibitory to surface expression. Under confocal microscopy, KRFX displayed patchy co-staining with cell surface receptor(s) and appeared to be located on the inner side of the plasma membrane. The 317-residue HIAx mutant that excised one additional lysine was much more impaired than the KRFX mutant. Still, the HIAx mutant exhibited some residual expression compared with the phenotype for the tailless  $\Delta 4$  mutant. The importance of the basic domain for plasma membrane interaction was further underscored by the contrasting phenotypes of CXCR4 chimeras with a WT or (+)  $\rightarrow$  A mutant CCR5 tail. Whereas surface expression of CXCR4 was not affected by replacement of its C-tail with that of WT CCR5, it was somewhat diminished for the chimera that exchanged the authentic CXCR4 tail for that of the (+)  $\rightarrow$  A CCR5 mutant.

On the basis of these results, we propose that the basic residue domain and the cysteine cluster constitute a bipartite motif critical for plasma membrane association (Fig. 11). The CCR5 tail chimera, which exchanged the CCR5 tail for that of CXCR4, was not expressed at the cell surface, perhaps due to the lack of this the bipartite motif. According to this model, the C-tail of CCR5 forms a fourth ICL in a sequential manner, first by electrostatic interaction between the basic domain and the polar head groups of phospholipids in the inner leaflet of the plasma membrane followed by *in situ* palmitoylation of the cysteine cluster that would reinforce this structure. This model differs from models proposed for similar motifs in N-terminal myristoylated proteins such as Src, HIV matrix, and Nef proteins (Fig. 11). In these cases, a basic domain stabilizes the poor plasma membrane binding of the myristyl group (83–85). Among the chemokine receptors, only CCR2B has a similar bipartite motif (Fig. 11). Consistent with this, a previous report showed that a CCR5/CCR2B chimera that substituted the third extracellular loop, seventh TM, and the cytoplasmic domain of CCR5 for that of CCR2B was competent for surface expression (86). Whether such a bipartite motif is a general requirement for normal trafficking of other GPCRs seems unlikely, since excision of this

motif from CCR2B did not affect surface expression (Fig. 6). However, the specificity of this motif for CCR5 could provide a selective target for anti-retroviral drug development.

**Acknowledgments**—We thank Alicia Buckler-White of NIAID (NIH) for oligonucleotide synthesis. We thank Owen Schwartz of the Biological Imaging Facility, RTB, NIAID (NIH) for technical advice on the use of the confocal microscope. We thank Eric Freed and Jonathan Silver of NIAID (NIH) and John Hanover of NIDDK (NIH) for discussion and comments. We are grateful to Nelson Cole of NHGRI (NIH) and Juan Bonifacio of CBMB, NICHD (NIH) for supplying Deng monoclonal antibody reactive with Golgi proteins and anti-mannosidase antibody, respectively. Finally, we acknowledge the contribution of several reagents by the NIH AIDS Research and Reference Reagent Program.

## REFERENCES

1. Boulay, F., Naik, N., Giannini, E., Tardif, M., and Bouchon, L. (1997) *Ann. N. Y. Acad. Sci.* **832**, 69–84
2. Combadiere, C., Ahuja, S. K., Tiffany, H. L., and Murphy, P. M. (1996) *J. Leukocyte Biol.* **60**, 147–152
3. Alkhatib, G., Combadiere, C., Broder, C. C., Feng, Y., Kennedy, P. E., Murphy, P. M., and Berger, E. A. (1996) *Science* **272**, 1955–1958
4. Deng, H., Liu, R., Ellmeier, W., Choe, S., Unutmaz, D., Burkhart, M., Di Marzio, P., Mamon, S., Sutton, R. E., Hill, C. M., Davis, C. B., Peiper, S. C., Schall, T. J., Littman, D. R., and Landau, N. R. (1996) *Nature* **381**, 661–666
5. Doranz, B. J., Rucker, J., Yi, Y., Smyth, R. J., Samson, M., Peiper, S. C., Parmentier, M., Collman, R. G., and Doms, R. W. (1996) *Cell* **85**, 1149–1158
6. Dragic, T., Litwin, V., Allaway, G. P., Martin, S. R., Huang, Y., Nagashima, K. A., Cavanan, C., Maddon, P. J., Koup, R. A., Moore, J. P., and Paxton, W. A. (1996) *Nature* **381**, 667–673
7. Murphy, P. M. (1994) *Annu. Rev. Immunol.* **12**, 593–633
8. Murphy, P. M. (1997) *Semin. Hematol.* **34**, 311–318
9. Sallusto, F., Mackay, C. R., and Lanzavecchia, A. (2000) *Annu. Rev. Immunol.* **18**, 593–620
10. Baldwin, J. M., Schertler, G. F., and Unger, V. M. (1997) *J. Mol. Biol.* **272**, 144–164
11. Ji, T. H., Grossmann, M., and Ji, I. (1998) *J. Biol. Chem.* **273**, 17299–17302
12. Wess, J. (1997) *FASEB J.* **11**, 346–354
13. Bockaert, J., and Pin, J. P. (1999) *EMBO J.* **18**, 1723–1729
14. Mellado, M., Rodriguez-Frade, J. M., Manes, S., and Martinez, A. C. (2001) *Annu. Rev. Immunol.* **19**, 397–421
15. Wong, L. M., Myers, S. J., Tsou, C. L., Gosling, J., Arai, H., and Charo, I. F. (1997) *J. Biol. Chem.* **272**, 1038–1045
16. Arai, H., Montecarlo, F. S., Tsou, C. L., Franci, C., and Charo, I. F. (1997) *J. Biol. Chem.* **272**, 25037–25042
17. Ben-Baruch, A., Bengali, K. M., Biragyn, A., Johnston, J. J., Wang, J. M., Kim, J., Chuntharapai, A., Michiel, D. F., Oppenheim, J. J., and Kelvin, D. J. (1995) *J. Biol. Chem.* **270**, 9121–9128
18. Mueller, S. G., White, J. R., Schraw, W. P., Lam, V., and Richmond, A. (1997) *J. Biol. Chem.* **272**, 8207–8214
19. Yang, W., Schraw, W. P., Mueller, S. G., and Richmond, A. (1997) *Biochemistry* **36**, 15193–15200
20. Cheng, Z. J., Zhao, J., Sun, Y., Hu, W., Wu, Y. L., Cen, B., Wu, G. X., and Pei, G. (2000) *J. Biol. Chem.* **275**, 2479–2485
21. Doranz, B. J., Orsini, M. J., Turner, J. D., Hoffman, T. L., Berson, J. F., Hoxie, J. A., Peiper, S. C., Brass, L. F., and Doms, R. W. (1999) *J. Virol.* **73**, 2752–2761
22. Haribabu, B., Richardson, R. M., Fisher, I., Sozzani, S., Peiper, S. C., Horuk, R., Ali, H., and Snyderman, R. (1997) *J. Biol. Chem.* **272**, 28726–28731
23. Hu, H., Shioda, T., Hori, T., Moriya, C., Kato, A., Sakai, Y., Matsushima, K., Uchiyama, T., and Nagai, Y. (1998) *Arch. Virol.* **143**, 851–861
24. Gonzalez, E., Bamshad, M., Sato, N., Mummidi, S., Dhand, R., Catano, G., Cabrera, S., McBride, M., Cao, X. H., Merrill, G., O'Connell, P., Bowden, D. W., Freedman, B. I., Anderson, S. A., Walter, E. A., Evans, J. S., Stephan, K. T., Clark, R. A., Tyagi, S., Ahuja, S. S., Dolan, M. J., and Ahuja, S. K. (1999) *Proc. Natl. Acad. Sci. U. S. A.* **96**, 12004–12009
25. Martin, M. P., Dean, M., Smith, M. W., Winkler, C., Gerrard, B., Michael, N. L., Lee, B., Doms, R. W., Margolick, J., Buchbinder, S., Goedert, J. J., O'Brien, T. R., Hilgartner, M. W., Vlahov, D., O'Brien, S. J., and Carrington, M. (1998) *Science* **282**, 1907–1911
26. McDermott, D. H., Zimmerman, P. A., Guignard, F., Kleiberger, C. A., Leitman, S. F., and Murphy, P. M. (1998) *Lancet* **352**, 866–870
27. Mummidi, S., Ahuja, S. S., Gonzalez, E., Anderson, S. A., Santiago, E. N., Stephan, K. T., Craig, F. E., O'Connell, P., Tryon, V., Clark, R. A., Dolan, M. J., and Ahuja, S. K. (1998) *Nat. Med.* **4**, 786–793
28. Kostrikis, L. G., Neumann, A. U., Thomson, B., Korber, B. T., McHardy, P., Karanikolas, R., Deutsch, L., Huang, Y., Lew, J. F., McIntosh, K., Pollack, H., Borkowsky, W., Spiegel, H. M., Palumbo, P., Oleske, J., Bardeguet, A., Luzuriaga, K., Sullivan, J., Wolinsky, S. M., Koup, R. A., Ho, D. D., and Moore, J. P. (1999) *J. Virol.* **73**, 10264–10271
29. Mummidi, S., Bamshad, M., Ahuja, S. S., Gonzalez, E., Feuillet, P. M., Begum, K., Galvis, M. C., Kostecki, V., Valente, A. J., Murthy, K. K., Haro, L., Dolan, M. J., Allan, J. S., and Ahuja, S. K. (2000) *J. Biol. Chem.* **275**, 18946–18961
30. Dean, M., Carrington, M., Winkler, C., Huttley, G. A., Smith, M. W., Allikmets, R., Goedert, J. J., Buchbinder, S. P., Vittinghoff, E., Gomperts, E., Donfield, S., Vlahov, D., Kaslow, R., Saah, A., Rinaldo, C., Detels, R., and O'Brien, S. J. (1996) *Science* **273**, 1856–1862
31. Huang, Y., Paxton, W. A., Wolinsky, S. M., Neumann, A. U., Zhang, L., He, T., Kang, S., Ceradini, D., Jin, Z., Yazdanbakhsh, K., Kunstman, K., Erickson,

- D., Dragon, E., Landau, N. R., Phair, J., Ho, D. D., and Koup, R. A. (1996) *Nat. Med.* **2**, 1240–1243
32. Benkirane, M., Jin, D. Y., Chun, R. F., Koup, R. A., and Jeang, K. T. (1997) *J. Biol. Chem.* **272**, 30603–30606
33. Wu, L., Paxton, W. A., Kassam, N., Ruffing, N., Rottman, J. B., Sullivan, N., Choe, H., Sodroski, J., Newman, W., Koup, R. A., and Mackay, C. R. (1997) *J. Exp. Med.* **185**, 1681–1691
34. Chen, Z., Kwon, D., Jin, Z., Monard, S., Telfer, P., Jones, M. S., Lu, C. Y., Aguilar, R. F., Ho, D. D., and Marx, P. A. (1998) *J. Exp. Med.* **188**, 2057–2065
35. Blanpain, C., Lee, B., Tackoen, M., Puffer, B., Boom, A., Libert, F., Sharron, M., Wittamer, V., Vassart, G., Doms, R. W., and Parmentier, M. (2000) *Blood* **96**, 1638–1645
36. Gosling, J., Monteclaro, F. S., Atchison, R. E., Arai, H., Tsou, C. L., Goldsmith, M. A., and Charo, I. F. (1997) *Proc. Natl. Acad. Sci. U. S. A.* **94**, 5061–5066
37. Doranz, B. J., Lu, Z. H., Rucker, J., Zhang, T. Y., Sharron, M., Cen, Y. H., Wang, Z. X., Guo, H. H., Du, J. G., Accavitti, M. A., Doms, R. W., and Peiper, S. C. (1997) *J. Virol.* **71**, 6305–6314
38. Alkhatib, G., Locati, M., Kennedy, P. E., Murphy, P. M., and Berger, E. A. (1997) *Virology* **234**, 340–348
39. Ansari-Lari, M. A., Liu, X. M., Metzker, M. L., Rut, A. R., and Gibbs, R. A. (1997) *Nat. Genet.* **16**, 221–222
40. Shioda, T., Nakayama, E. E., Tanaka, Y., Xin, X., Liu, H., Kawana-Tachikawa, A., Kato, A., Sakai, Y., Nagai, Y., and Iwamoto, A. (2001) *J. Virol.* **75**, 3462–3468
41. Blanpain, C., Wittamer, V., Vanderwinden, J. M., Boom, A., Renneboog, B., Lee, B., Le Poul, E., El Asmar, L., Govaerts, C., Vassart, G., Doms, R. W., and Parmentier, M. (2001) *J. Biol. Chem.* **276**, 23795–23804
42. Ahuja, S. K., Lee, J. C., and Murphy, P. M. (1996) *J. Biol. Chem.* **271**, 225–232
43. Alkhatib, G., Berger, E. A., Murphy, P. M., and Pease, J. E. (1997) *J. Biol. Chem.* **272**, 20420–20426
44. Combadiere, C., Ahuja, S. K., and Murphy, P. M. (1995) *J. Biol. Chem.* **270**, 16491–16494; Correction (1996) *J. Biol. Chem.* **271**, 11034
45. Venkatesan, S., Gerstberger, S. M., Park, H., Holland, S. M., and Nam, Y. (1992) *J. Virol.* **66**, 7469–7480
46. Farzan, M., Mirzabekov, T., Kolchinsky, P., Wyatt, R., Cayabyab, M., Gerard, N. P., Gerard, C., Sodroski, J., and Choe, H. (1999) *Cell* **96**, 667–676
47. Brodsky, J. L., and McCracken, A. A. (1999) *Semin. Cell Dev. Biol.* **10**, 507–513
48. Kopito, R. R. (1997) *Cell* **88**, 427–430
49. Plemper, R. K., and Wolf, D. H. (1999) *Mol. Biol. Rep.* **26**, 125–130
50. Petaja-Repo, U. E., Hogue, M., Laperriere, A., Walker, P., and Bouvier, M. (2000) *J. Biol. Chem.* **275**, 13727–13736
51. Petaja-Repo, U. E., Hogue, M., Laperriere, A., Bhalla, S., Walker, P., and Bouvier, M. (2001) *J. Biol. Chem.* **276**, 4416–4423
52. Jockers, R., Angers, S., Da Silva, A., Benaroch, P., Strosberg, A. D., Bouvier, M., and Marullo, S. (1999) *J. Biol. Chem.* **274**, 28900–28908
53. Obin, M. S., Jahngen-Hodge, J., Nowell, T., and Taylor, A. (1996) *J. Biol. Chem.* **271**, 14473–14484
54. Abeijon, C., and Hirschberg, C. B. (1987) *J. Biol. Chem.* **262**, 4153–4159
55. Bosshart, H., Straehl, P., Berger, B., and Berger, E. G. (1991) *J. Cell. Physiol.* **147**, 149–156
56. Hanover, J. A., Elting, J., Mintz, G. R., and Lennarz, W. J. (1982) *J. Biol. Chem.* **257**, 10172–10177
57. Sadeghi, H., and Birnbaumer, M. (1999) *Glycobiology* **9**, 731–737
58. Rottger, S., White, J., Wandall, H. H., Olivo, J. C., Stark, A., Bennett, E. P., Whitehouse, C., Berger, E. G., Clausen, H., and Nilsson, T. (1998) *J. Cell Sci.* **111**, 45–60
59. Roth, J., Wang, Y., Eckhardt, A. E., and Hill, R. L. (1994) *Proc. Natl. Acad. Sci. U. S. A.* **91**, 8935–8939
60. Roth, J. (1984) *J. Cell Biol.* **98**, 399–406
61. Munro, S. (1995) *EMBO J.* **14**, 4695–4704
62. Nilsson, T., Slusarewicz, P., Hoe, M. H., and Warren, G. (1993) *FEBS Lett.* **330**, 1–4
63. Nilsson, T., and Warren, G. (1994) *Curr. Opin. Cell Biol.* **6**, 517–521
64. Munro, S. (1998) *Trends Cell Biol.* **8**, 11–15
65. Locker, J. K., Klumperman, J., Oorschot, V., Horzinek, M. C., Geuze, H. J., and Rottier, P. J. (1994) *J. Biol. Chem.* **269**, 28263–28269
66. Locker, J. K., Opstelten, D. J., Ericsson, M., Horzinek, M. C., and Rottier, P. J. (1995) *J. Biol. Chem.* **270**, 8815–8821
67. Weisz, O. A., Swift, A. M., and Machamer, C. E. (1993) *J. Cell Biol.* **122**, 1185–1196
68. Nilsson, T., Hoe, M. H., Slusarewicz, P., Rabouille, C., Watson, R., Hunte, F., Watzel, G., Berger, E. G., and Warren, G. (1994) *EMBO J.* **13**, 562–574
69. Nickel, W., Brugger, B., and Wieland, F. T. (1998) *Semin. Cell Dev. Biol.* **9**, 493–501
70. Nathans, J. (1992) *Biochemistry* **31**, 4923–4931
71. Latronico, A. C., and Segaloff, D. L. (1999) *Am. J. Hum. Genet.* **65**, 949–958
72. Oksche, A., and Rosenthal, W. (1998) *J. Mol. Med.* **76**, 326–337
73. Sung, C. H., Makino, C., Baylor, D., and Nathans, J. (1994) *J. Neurosci.* **14**, 5818–5833
74. Schulein, R., Hermosilla, R., Oksche, A., Dehe, M., Wiesner, B., Krause, G., and Rosenthal, W. (1998) *Mol. Pharmacol.* **54**, 525–535
75. Baker, E. K., Colley, N. J., and Zuker, C. S. (1994) *EMBO J.* **13**, 4886–4895
76. Colley, N. J., Baker, E. K., Stamnes, M. A., and Zuker, C. S. (1991) *Cell* **67**, 255–263
77. Ferreira, P. A., Hom, J. T., and Pak, W. L. (1995) *J. Biol. Chem.* **270**, 23179–23188
78. Ferreira, P. A., Nakayama, T. A., Pak, W. L., and Travis, G. H. (1996) *Nature* **383**, 637–640
79. Dwyer, N. D., Troemel, E. R., Sengupta, P., and Bargmann, C. I. (1998) *Cell* **93**, 455–466
80. Evans, B. N., Rosenblatt, M. I., Mnayer, L. O., Oliver, K. R., and Dickerson, I. M. (2000) *J. Biol. Chem.* **275**, 31438–31443
81. White, J. H., Wise, A., Main, M. J., Green, A., Fraser, N. J., Disney, G. H., Barnes, A. A., Emson, P., Foord, S. M., and Marshall, F. H. (1998) *Nature* **396**, 679–682
82. Bultmann, A., Muranyi, W., Seed, B., and Haas, J. (2001) *J. Virol.* **75**, 5263–5276
83. Hermida-Matsumoto, L., and Resh, M. D. (1999) *J. Virol.* **73**, 1902–1908
84. Resh, M. D. (1994) *Cell* **76**, 411–413
85. Welker, R., Harris, M., Cardel, B., and Krausslich, H. G. (1998) *J. Virol.* **72**, 8833–8840
86. Rucker, J., Samson, M., Doranz, B. J., Libert, F., Berson, J. F., Yi, Y., Smyth, R. J., Collman, R. G., Broder, C. C., Vassart, G., Doms, R. W., and Parmentier, M. (1996) *Cell* **87**, 437–446